

Table 1  
 $A_z$  values for 16 radiologists for interpretation without and with CAD scheme

Radiologist	Without CAD scheme	With CAD scheme
<i>Chest</i>		
A	0.763	0.871
B	0.833	0.844
C	0.823	0.840
D	0.768	0.819
E	0.840	0.883
F	0.849	0.857
G	0.757	0.833
Mean	0.805	0.850
<i>General</i>		
H	0.798	0.871
I	0.736	0.898
J	0.793	0.837
K	0.790	0.861
L	0.706	0.874
M	0.695	0.812
N	0.826	0.881
O	0.781	0.826
P	0.807	0.835
Mean	0.770	0.855
Mean for all	0.785	0.853

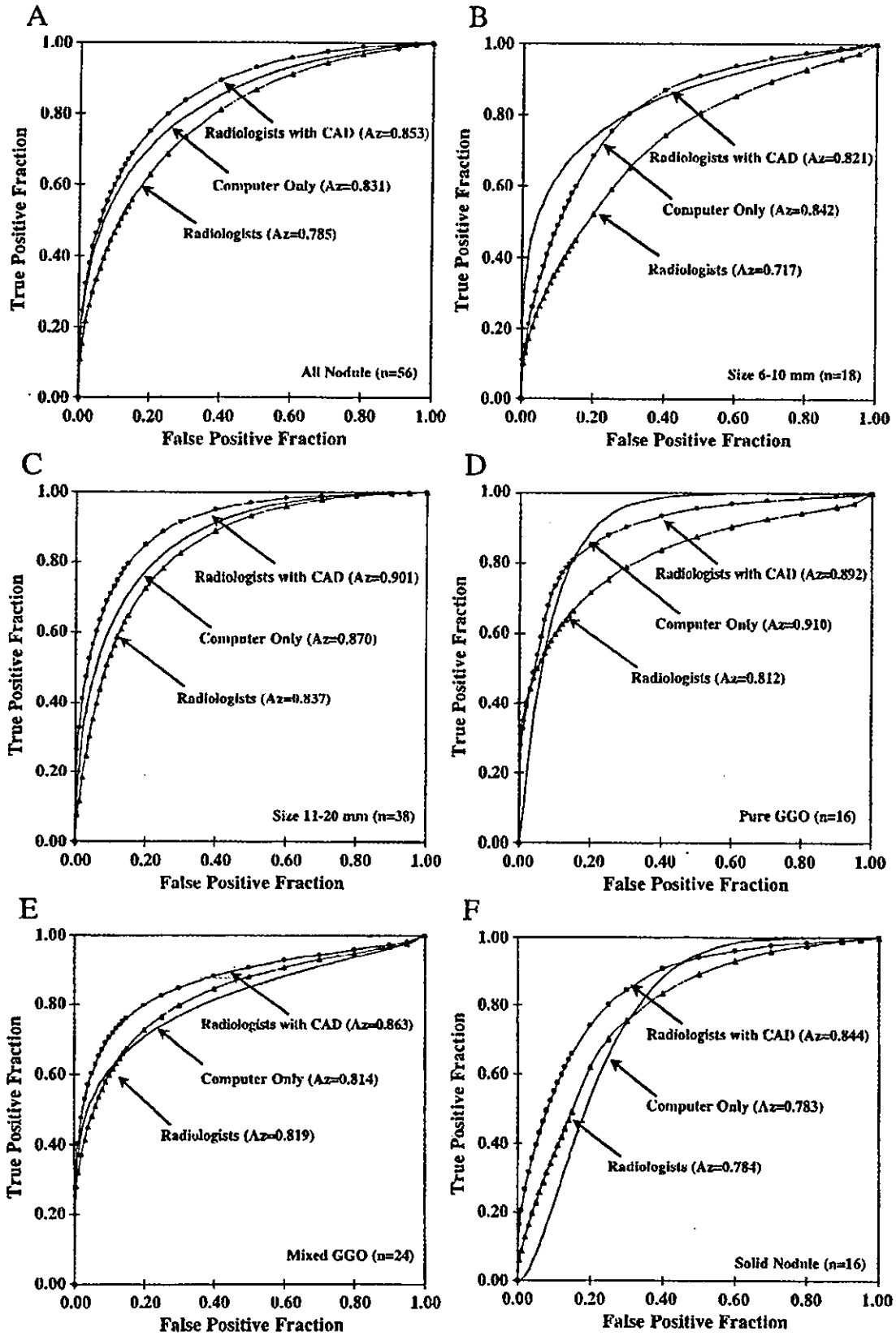
The difference was statistically significant with a  $p$  value 0.01 for general radiologists (0.12 for chest radiologists) between radiologist without and with CAD scheme. No statistically significant difference was found between chest and general radiologists for each condition without and with CAD scheme.

selected from 183 benign nodules matched in size and pattern to the cancers. Sixteen radiologists participated in this study.

A number of axial images for each nodule on HRCT were displayed for interpretation in cine mode on a CRT monitor. For a training session before the test, we provided five different cases so that the observers could learn how to operate the cine mode interface and how to take into account the computer output in their decision. We informed observers that the sensitivity and specificity of our CAD scheme, using a threshold of 0.50 (50%) for the likelihood of malignancy, were 80% and 75%, respectively. The images were presented to radiologists, first without and then with the computer output, who were asked to indicate their confidence level regarding the malignancy of a nodule.

The performance ( $A_z$ ) of the CAD scheme was 0.831 in the distinction between the 28 malignant and 28 benign nodules used in this observer study. The average  $A_z$  value for the 16 radiologists was improved from 0.785 to 0.853 by a statistically significant level ( $P=0.02$ ) with the aid of the CAD scheme for the 56 nodules.

Fig. 1. ROC curves show the performance of the computer alone and the average performance of 16 radiologists without and with CAD scheme for two size and three pattern groups. (A) All nodules, (B) small nodules, (C) large nodules, (D) pure GGO, (E) mixed GGO, (F) solid nodules.



#### 2.4. Different groups

The 16 radiologists were divided into two groups, which included seven chest radiologists with the mean experience of 15 years and nine general radiologists with the mean experience of 13 years. The 56 nodules included two groups of nodules of different size (9 small nodules of 6–10 mm and 19 large nodules of 11–20 mm), and also three groups with different patterns (8 nodules with pure GGO, 12 nodules with mixed GGO, and 8 solid nodules) for both malignant and benign lesions.

#### 2.5. Data analysis

The confidence level ratings by each observer were analyzed by use of receiver operating characteristic (ROC) methodology, and a quasi-maximum likelihood estimation of the binormal distribution was fitted to the radiologists' confidence ratings [7]. The statistical significance of the difference in  $A_z$  values between observer readings without and with the CAD scheme was tested by use of the Dorfman–Berbaum–Metz method [8], which included both reader variation, and case sample variation by means of an analysis-of-variance approach.

### 3. Results

The  $A_z$  values for radiologists without and with the CAD scheme were improved from 0.770 to 0.855 for the nine general radiologists ( $P=0.01$ ), and from 0.805 to 0.850 for the seven chest radiologists ( $P=0.12$ ).  $A_z$  values without and with the CAD scheme for each radiologist are listed in Table 1.

The  $A_z$  values of the classification CAD scheme were 0.842 for small nodules, 0.870 for large nodules, 0.910 for nodules with pure GGO, 0.814 for nodules with mixed GGO, and 0.783 for solid nodules. The  $A_z$  values for radiologists without and with the CAD scheme were improved from 0.717 to 0.821 for small nodules ( $P=0.04$ ) and from 0.837 to 0.901 for large nodules ( $P=0.04$ ); and from 0.812 to 0.892 for nodules with pure GGO ( $P=0.149$ ), from 0.819 to 0.863 for nodules with mixed GGO ( $P=0.196$ ), and from 0.784 to 0.844 for solid nodules ( $P=0.334$ ). ROC curves for use of the computer alone and the average performance of 16 radiologists without and with the CAD scheme for distinction between malignant and benign nodules are shown in Fig. 1 (two size and three pattern groups).

### 4. Conclusion

CAD has the potential to improve the diagnostic accuracy in distinguishing benign nodules from malignant ones in different groups on HRCT.

### Acknowledgements

The authors are grateful to Takeshi Kobayashi, MD, Kazuto Ashizawa, MD, Naohiro Matsuyama, MD, Hajime Abiru, MD, Tetsuji Yamaguchi MD, Chaotong Zhang, MD, Peter MacEaney, MD, Ulrich Bick, MD, Christopher Straus, MD, Edward Michals, MD, Gregory Scott Stacy, MD, Akiko Egawa, MD, Tomoaki Okimoto, MD, Kazunori Minami,

MD, and Shuji Sakai, MD, for participating as observers; and to Shigehiko Katsuragawa, PhD, for helpful suggestions. This work was partly supported by USPHS grants CA62625 and CA 98119. H. MacMahon and K. Doi are shareholders of R2 Technology, Los Altos, CA. K. Doi is a shareholder of Deus Technology, Rockville, MD.

## References

- [1] S. Sone, et al., Mass screening for lung cancer with mobile spiral computed tomography scanner, *Lancet* 351 (1998) 1242-1245.
- [2] C.I. Henschke, et al., Early lung cancer action project: overall design and findings from baseline screening, *Lancet* 354 (1999) 99-105.
- [3] S. Diederich, et al., Screening for early lung cancer with low-dose spiral CT: prevalence in 817 asymptomatic smokers, *Radiology* 222 (2002) 773-781.
- [4] C.I. Henschke, et al., CT screening for lung cancer: frequency and significance of part-solid and nonsolid nodules, *AJR* 178 (2002) 1053-1057.
- [5] F. Li, Comparison of thin section CT findings in malignant and benign nodules in CT screening for lung cancer, *Radiology* (in press).
- [6] F. Li, et al., Improvement in radiologists' performance for differentiating small benign from malignant lung nodules on high-resolution CT by using computer-estimated likelihood of malignancy, *AJR* (in press).
- [7] C.E. Metz, B.A. Herman, J.H. Shen, Maximum-likelihood estimation of receiver operating (ROC) curves from continuously distributed data, *Stat. Med.* 17 (1998) 1033-1053.
- [8] D.D. Dorfman, K.S. Berbaum, C.E. Metz, ROC rating analysis: generalization to the population of readers and cases with the jackknife method, *Invest. Radiol.* 27 (1992) 723-731.

---

# Effect of Temporal Subtraction Images on Radiologists' Detection of Lung Cancer on CT: Results of the Observer Performance Study with Use of Film Computed Tomography Images<sup>1</sup>

Hiroyuki Abe, MD, PhD, Takayuki Ishida, PhD, Junji Shiraishi, PhD, Feng Li, MD, PhD, Shigehiko Katsuragawa, PhD, Shusuke Sone, MD, Heber MacMahon, MD, Kunio Doi, PhD

---

**Rationale and Objectives.** To evaluate the effect of temporal subtraction images on the radiologists' detection of early primary lung cancer in computed tomography (CT) scans.

**Materials and Methods.** Fourteen cases with primary lung cancer and 16 normal cases were used for this study from a database of low-dose CT images, which were obtained from a lung cancer screening program in Nagano, Japan. Images were obtained with a single-detector helical CT scanner using 10 mm collimation and 2:1 pitch. Each case had both previous and current CT scans. Temporal subtraction images were obtained by subtracting the warped previous images from the current images. Seven radiologists, including four attendings and three residents, provided their confidence levels for the presence or absence of lung cancers with use of film CT images without and with temporal subtraction images. Receiver operating characteristic analysis was used to compare their performance without and with temporal subtraction images.

**Results.** The mean Az values (area under the receiver operating characteristic curve) of seven observers without and with temporal subtraction images were 0.868 and 0.930, respectively. Diagnostic accuracy was significantly improved by using temporal subtraction images ( $P = .007$ ). Temporal subtraction images were especially useful when a nodule was present near the pulmonary hilum, where radiologists tended to overlook it.

**Conclusion.** The temporal subtraction technique can significantly improve the sensitivity and specificity for detection of lung cancer on CT scans.

**Key Words.** Lung cancer; temporal subtraction; computed tomography (CT); computer-aided diagnosis (CAD); observer study.

© AUR, 2004

---

Acad Radiol 2004; 11:1337-1343

<sup>1</sup> From Kurt Rossmann Laboratories for Radiologic Image Research, Department of Radiology, The University of Chicago, MC 2026, 5841 S Maryland Ave, Chicago, IL 60637 (H.A., J.S., F.L., H.M., K.D.); Hiroshima International University, Hiroshima, Japan (T.I.); Kumamoto University, Kumamoto, Japan (S.K.); and Azumi General Hospital, Nagano, Japan (S.S.). Received May 16, 2004; revision requested June 24; received July 6; revision requested August 10; received August 27; accepted August 29. Supported by US Public Health Service grant no. CA62625. Address correspondence to H.A. e-mail: habe@uchicago.edu

© AUR, 2004

doi:10.1016/j.acra.2004.08.010

Screening for lung cancer with low-dose computed tomography (CT) has become popular in the United States and Japan, partly because earlier-stage cancer can be detected with CT than with chest radiographs (1,2). However, radiologists sometimes overlook lung cancer even with CT, despite the fact that CT has high spatial and contrast resolution (3-5).

A temporal subtraction technique for chest radiographs, in which areas of interval change were enhanced by using the previous radiograph as a subtraction mask, has been developed previously (6-8). The observer study confirmed that the temporal subtraction technique was helpful

to radiologists in the detection of subtle nodules which might have been missed without it (9–11). To our knowledge, there has been no report published regarding the use of temporal subtraction for CT. The purpose of this study is to report the results of an observer study conducted to determine if a temporal subtraction technique could be useful to improve the accuracy of radiologists in detecting subtle nodules caused by lung cancer on CT.

**MATERIALS AND METHODS**

**Cases**

We selected 14 cases with primary lung cancer and 16 normal cases for this study from a database of low-dose CT images, which were obtained from a CT screening program for lung cancer conducted in Nagano, Japan, from 1996 to 1999. The database consists of 7,847 screenees including 87 cases with primary lung cancer. In the screening program, all subjects gave informed consent. All cases used in this study had at least two sequential CT images with from 1- to 2-year interval between them. All of the CT images were obtained with a single detector helical CT scanner (W950SR; Hitachi Medical, Tokyo, Japan) with a 10 mm collimation and one rotation of the x-ray tube per 2-seconds with table speed of 10 mm/sec (pitch; 2:1). All of the scans were performed in a 32-second breath hold with scanning from below the level of diaphragm to above the level of apex. All of the images were reconstructed as 10 mm slice thickness. Although the number of slices obtained in these cases was 32, all of cases used in this study covered the entire lungs within 30 slices.

The selection criteria for positive cases included solitary, primary lung cancer and cases having at least two sequential CT scans with growth of a nodule observed in the latter CT. The size of the nodules ranged from 5–24 mm (mean, 12 mm). The normal cases were selected randomly without the knowledge of the quality of subtraction images produced. All of the normal cases were verified by three experienced radiologists (H.A, F.L, H.M), who did not participate in the observer study, for the absence of nodules or nodule-like lesions.

The location of the tumor was categorized into three areas; peripheral lung field, central lung field, and perihilum. When the tumor was located within 2 cm from the pulmonary hilum, the location of the tumor was determined as perihilum. In the same manner, when the tumor was located in the lung field within 2 cm from the pleura,

**Table 1**  
**A<sub>z</sub> Value of Each Observer in the Detection of Lung Cancer Without and With Temporal Subtraction Image**

		Without	With
Attending	A	0.810	0.949
	B	0.861	0.932
	C	0.905	0.928
	D	0.858	0.943
	mean	0.858	0.938
Residents	E	0.933	0.965
	F	0.757	0.812
	G	0.955	0.983
	mean	0.882	0.920
All	mean	0.868	0.930

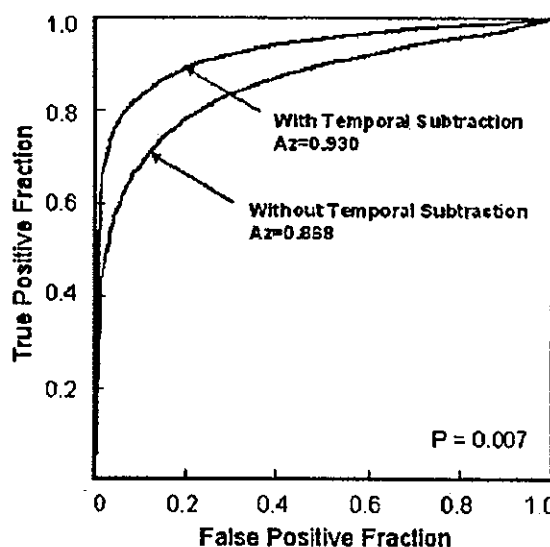


**Figure 1.** ROC curves for the average performance of seven observers in the detection of lung cancer on CT without and with temporal subtraction. The performance with temporal subtraction is significantly higher than that without it ( $P = .007$ ).

the location of the tumor was determined as peripheral lung field. (If the tumor was located within 2 cm both from the pulmonary hilum and from the pleura, the location of the tumor was determined as perihilum.) The location of the remaining tumors was determined as in central lung field.

Primary cancers consisted of adenocarcinoma ( $n = 9$ ), small cell carcinoma ( $n = 3$ ), and squamous cell carcinoma ( $n = 2$ ). Of these cancers, eight represented ground glass opacity and six showed solid opacity. The average age of the patients was 69.6 for cases with cancer (range, 56–89), and 51.4 for normal cases (range, 44–74).

**Table 2**  
**The Number of Beneficial and Detrimental Effects in Both Normal and Cancer Cases**

		Beneficial effect			Detrimental effect		
		Normal	Cancer	Total	Normal	Cancer	Total
Attendings	A	11	2	13	1	1	2
	B	1	2	3	0	0	0
	C	6	1	7	1	2	3
	D	13	2	15	1	2	3
Residents	E	7	1	8	0	1	1
	F	6	2	8	0	2	2
	G	4	0	4	0	0	0
	mean	6.9	1.4	8.3	0.4	1.2	1.6

### Temporal Subtraction Technique

The temporal subtraction technique on chest radiographs has been described in detail previously (6–8). In this study, we used an initial version of the temporal subtraction scheme to create the subtraction images. In the scheme, the selection of the corresponding section in the two sets of CT images and image shift correction between the current and the previous image were performed manually.

For making a subtraction of CT image in each slice, we used an iterative image warping technique. First, a number of template regions of interests (ROIs) with a  $32 \times 32$  matrix size and the corresponding search area ROIs with a  $64 \times 64$  matrix size were selected automatically on the previous and current images, respectively. Then, the shift values for template ROIs, which would match to the corresponding areas in search area ROIs were determined for all pairs of selected ROIs by means of a cross-correlation technique. The previous image was nonlinearly warped according to local shift vectors for "best-matching," which was determined by highest cross-correlation value (6,12–14). The warped previous image was then used for the second warping for further reduction of misregistration artifacts. Finally, the temporal subtraction image was obtained by subtracting the second warped previous image from the current image.

### Observer Test and Data Analysis

Four attending radiologists (years of experience, 6–16; mean, 12.0 years) and three radiology residents (one third-year, and two fourth-year residents) participated in the observer study. Before the test, the observers were told that about half of the cases had solitary lung cancer and the rest were normal and that the benign lesions such

as scar, atelectasis, and interstitial opacities should be ignored. For a training session, four cases (two cancer cases and two normal cases) were presented for each observer to become familiar with the test. In the test, observers were required to indicate their diagnostic decisions without temporal subtraction images initially, and then with temporal subtraction images, sequentially. All the slice images for previous CT, current CT, and the subtraction technique were printed separately on  $14 \times 17$  inch films (capable of having 30 slice images maximum) with a window width of 1,500 Hounsfield unit (HU) and a window level of  $-700$  HU.

Observers indicated their confidence levels regarding the presence or absence of cancers using an analog continuous-rating scale with a line-checking method. There were two identical 7-cm-long lines arranged one above the other, with about 5 mm distance in between. For the initial ratings, the observers marked their confidence levels along the upper line. Points toward the right or left end of the bar indicated the observer's greater confidence in a positive or negative result, respectively. Only when the second ratings were different from the initial ratings, observers indicated their confidence levels in the lower line. Test sequence is as follows; previous and current CT images were presented to observers, who were asked to indicate their confidence rating without temporal subtraction first. Immediately after the completion of initial rating, temporal subtraction images were presented together with those previous and current CT images, and observers were given the opportunities to change their confidence ratings. There was no time limit for the test. In the test, no observer requested a break, and the average time for each reading session was approximately 1 hour.

**Table 3**  
The Number of Observers Who Detected the Cancer Without and With Temporal Subtraction, and the Size and Location of the Cancer

Case No.	Size (mm)	Location*	Detected without temporal subtraction	Missed Initially, but detected with the aid of temporal subtraction
1	21	perihilum, rt	1	6
2	6	peripheral, lt	1	0
3	10	peripheral, lt	2	0
4	5	peripheral, rt.	2	0
5	8	central, lt	3	1
6	10	perihilum, rt	4	0
7	11	perihilum, lt.	5	2
8	21	central, rt	6	0
9	15	peripheral, lt	6	0

\*peripheral: peripheral lung field; central: central lung field

The observer performance in the detection of lung cancer, without and with temporal subtraction, was evaluated by means of receiver operating characteristic (ROC) analysis. A binormal ROC curve was fitted to each observer's confidence rating data by using the maximum likelihood estimation (15). A computer program, LABROC5, was used for obtaining binormal ROC curves by use of the confidence level scored by measuring the distance from the left end of the line to the marked point on the continuous-rating scale and converting the measurement to a scale from 0.00 to 1.00. The  $A_z$  value was calculated for each fitted curve. The statistical significance of the difference between the  $A_z$  values obtained without and with the aid of temporal subtraction images was tested by use of the paired *t*-test.

We assumed that the temporal subtraction technique had a clinically relevant effect on an observer's diagnosis when there was a difference in the rating scores of 30% or more between the first and second ratings. We also assumed that the temporal subtraction technique was beneficial only when the second rating was on the point more than half of the continuous-rating scale toward the correct end, in addition to the 30% change in the confidence level. The temporal subtraction technique was detrimental when there was a 30% change toward the incorrect end of the continuous-rating scale. We assumed that the cancer was overlooked by the observer when the rating of confidence level was less than 0.5 in positive cases. The statistical significance of the difference in these results was tested by use of the paired *t*-test.

## RESULTS

The results of the observer's performance without and with temporal subtraction images are shown in Table 1.

All observers improved their performance in the detection of lung cancer by using temporal subtraction images. The average area under the ROC curve ( $A_z$  value) for seven observers was significantly improved by using the temporal subtraction technique, from 0.868 to 0.930 ( $P = .007$ ) (Fig 1). Table 2 shows the beneficial and detrimental effect of the temporal subtraction on each observer. The average number of cases for beneficial effect was significantly ( $P = .006$ ) greater than that for detrimental effect. The beneficial effect was appreciated significantly ( $P = .009$ ) more in normal cases than in cancer cases.

Five cancers (case No. 2-6) were not detected by at least three observers both without and with temporal subtraction (Table 3). Of these five cancers, all cancers measured within 10 mm and three cancers located in peripheral lung field. Two cancers (case No. 1, 7) were overlooked by multiple observers initially, but were detected with the aid of temporal subtraction (Table 3). Those two cancers were located at perihilum (Fig 2).

## DISCUSSION

Subtle nodules and nodules overlapped with normal structures or located near the large vessels are likely to be "missed nodules" on CT (16). Because the temporal subtraction technique can remove most of the normal structures from the images, it appears appropriate to use this technique for detection of nodules which are obscured by the normal structures (10). Observers tended to overlook nodules located at perihilum without temporal subtraction in this study, in spite of the fact that radiologists might be expected to detect lesions more sensitively in an observer test than in daily clinical work, because the task in an





**Figure 2.** Case 1 (a, previous CT; b, current CT; c, temporal subtraction image): A lung cancer located behind the right pulmonary hilum on the current CT image (b, curved arrow). At the same section on the previous CT, there is only a small, faint opacity at the same location (a, arrow). Temporal subtraction clearly demonstrates the new nodule as a dark area that stands out from the gray background (c). Six of seven observers missed this lesion initially, but detected it after viewing the temporal subtraction image.

observer test is simplified and the observer is not subject to interruptions. In this study, temporal subtraction images clearly helped the radiologists not to miss cancers at least in two cases (Fig 2). On the other hand, small cancers located in the periphery tended to be overlooked even with temporal subtraction, partly because the lesions in the subtraction images were sometimes obscured by the artifacts caused by misregistration the normal structures (Fig 3). The detectability of these small cancers may be improved, if misregistration artifacts in the subtraction images can be reduced in the future. Despite these artifacts, however, only a small number of detrimental effects were found with use of the temporal subtraction. This is likely because the temporal subtraction images are only used as a guide to direct attention to suspicious area in the original images. If the opacity on the subtraction image is not confirmed on the original image, it is assumed to be an artifact. As to the beneficial effect, it tended to

be greater in normal cases, to confirm the absence of new nodule, than in cancer cases. This could bring great benefit if temporal subtraction were used in a screening program where the majority of examinations are normal.

In this study, we used films, not a soft copy display, to show CT images for the observers. Although cine mode soft copy viewing of spiral CT images of the chest may improve the radiologists' ability to detect nodules compared with hard copy reading (17), we believe that the radiologists' performance would be improved with temporal subtraction even if a cine viewing were used because lung cancers was commonly overlooked even with soft copy displays (3).

The observer performance test is usually conducted in two ways (ie, an independent test and a sequential test). The independent test consists of two separate sessions to obtain results without and with aid independently. The sequential test is conducted in one session in which

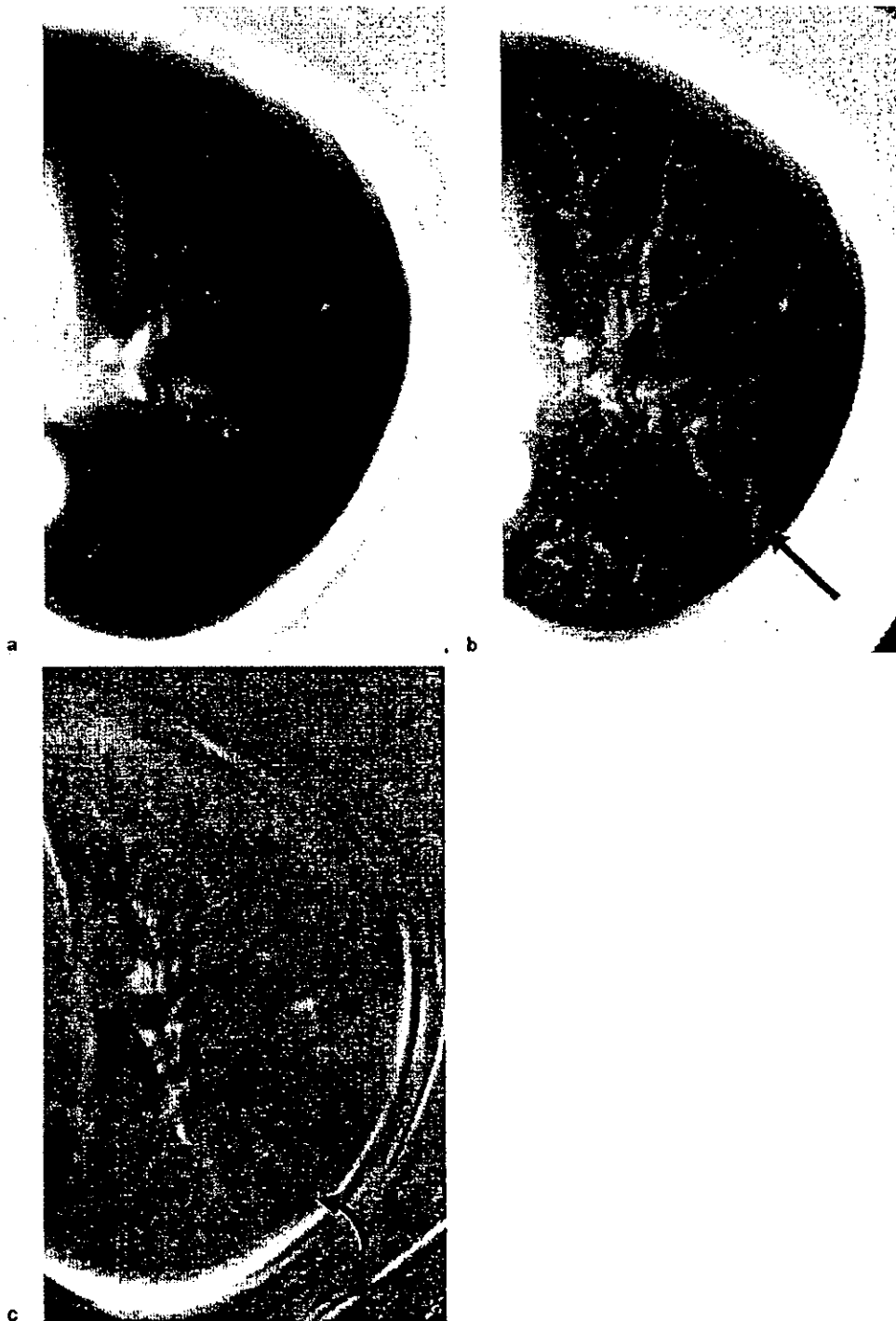


**Figure 3.** Case 2 (a, previous CT; b, current CT; c, temporal subtraction image). A small lung cancer is located in the left peripheral lung field (b, arrow). Although temporal subtraction image depicts a small cancer (c, curved arrow), misregistration artifacts around the bronchovascular bundle detract from the conspicuity of the lesion.

images without and with aid are shown sequentially. Kobayashi et al (18) and Uozumi et al (10) reported that there were no statistically significant differences in the Az values obtained with the two test methods. In the current study, we used the sequential test because it is more efficient and convenient.

The ROC analysis is a statistically sophisticated way to evaluate the observer performance test. However, the difference in Az values would sometimes be difficult for clinicians to feel its impact for their work. Therefore, some investigators have analyzed the beneficial and detrimental effects by setting the cut-off point on the confidence ratings (10,18–21). The cut-off point is usually set arbitrarily. We believe that this analysis would provide some sense of clinical relevance, if the cut-off point is selected carefully. We selected the cut-off point as 0.5 in the current study. We believe that the cut-off point of 0.5 would be reasonable because the observers were told to use the line for confidence rating uniformly from the point 0 to 1.0, according to their confidence level.

Although we obtained statistically significant differences in observers' performances between without and with temporal subtraction, these results were obtained from a relatively small number of cases (30 cases) with a small number of observers (seven observers). To verify these results, a larger scale of observer test would be warranted.

In conclusion, temporal subtraction may be useful with CT images to improve the diagnostic performance of radiologists in the detection of lung cancer.

#### REFERENCES

1. Patz EF, Goodman PC, Bepko G. Screening for lung cancer. *N Engl J Med* 2000; 343:1627–1633.
2. Henschke CI, McCauley DI, Yankelevitz DF, et al. Early Lung Cancer Action Project: A summary of the findings on baseline screening. *Oncologist* 2001; 6:147–152.
3. Kakimura R, Ohmatsu H, Kaneko M, et al. Detection failures in spiral CT screening for lung cancer: Analysis of CT findings. *Radiology* 1999; 212:61–66.
4. White CS, Romney BM, Mason AC, et al. Primary carcinoma of the lung overlooked at CT: Analysis of findings in 14 patients. *Radiology* 1996; 199:109–115.
5. Gurney JW. Missed lung cancer at CT: imaging findings in nine patients. *Radiology* 1996; 199:117–122.
6. Kano A, Doi K, MacMahon H, et al. Digital image subtraction of temporally sequential chest images for detection of interval change. *Med Phys* 1994; 21:453–461.
7. Ishida T, Ashizawa K, Engelmann R, et al. Application of temporal subtraction for detection of interval change in chest radiographs: Improvement of subtraction image using automated initial image matching. *J Dig Imaging* 1999; 12:77–86.
8. Ishida T, Katsuragawa S, Nakamura K, et al. Iterative image warping technique for temporal subtraction of sequential chest radiographs to detect interval change. *Med Phys* 1999; 26:1320–1329.
9. Difazio MC, MacMahon H, Xu XW, et al. Effect of time interval difference images on detection accuracy in digital chest radiography. *Radiology* 1997; 202:447–452.
10. Uozumi T, Nakamura K, Watanabe H, et al. ROC analysis on detection of metastatic pulmonary nodules on digital chest radiographs by use of temporal subtraction. *Acad Radiol* 2001; 8:871–878.
11. Johkoh T, Kozuka T, Tomiyama N, et al. Temporal subtraction for detection of solitary pulmonary nodules on chest radiographs: Evaluation of a commercially available computer-aided diagnosis system. *Radiology* 2002; 223:806–811.
12. Lillestrand, RL, Hoyt RR. The design of advanced digital image processing systems. *Photogramm Eng* 1974; 40:1201–1217.
13. Lillestrand, RL. Techniques for change detection. *IEEE Trans C* 1972; 21:654–659.
14. Ustlad MS. An algorithm for estimating small scale differences between two digital images. *Pattern Recognition* 1973; 5:323–333.
15. Metz CE, Herman BA, Shen J-H. Maximum-likelihood estimation of receiver operating characteristic (ROC) curves from continuously distributed data. *Stat Med* 1998; 17:1033–1053.
16. Li F, Sone S, Abe H, et al. Missed lung cancers in low-dose helical CT screening obtained from a general population. *Radiology* 2002; 225: 673–683.
17. Seltzer SE, Judy PF, Adams DF, et al. Spiral CT of the chest: comparison of cine and film-based viewing. *Radiology* 1995; 197:73–78.
18. Kobayashi T, Xu XW, MacMahon H, et al. Effect of a computer-aided diagnosis scheme on radiologists' performance in detection of lung nodules on radiographs. *Radiology* 1996; 199:843–848.
19. Kakeda S, Nakamura K, Kamada K, et al. Improved detection of lung nodules by using a temporal subtraction technique. *Radiology* 2002; 224:145–151.
20. Tsukuda S, Heshiki A, Katsuragawa S, et al. Detection of lung nodules on digital chest radiographs: Potential usefulness of a new contralateral subtraction technique. *Radiology* 2002; 223:199–203.
21. Ashizawa K, MacMahon H, Ishida T, et al. Effect of an artificial neural network on radiologists' performance in the differential diagnosis of interstitial lung disease using chest radiographs. *AJR Am J Roentgenol* 1999; 172:1311–1315.

## Pulmonary Lesions Detected in Population-based CT Screening for Lung Cancer: Reliable Findings of Benign Lesions

Tadashi Murakami, Yoshifumi Yasuhara, Shinji Yoshioka, Masahiko Uemura, Teruhito Mochizuki, and Junpei Ikezoe

**Purpose:** To identify the characteristics of benign pulmonary lesions in order to reduce false-positive rates in screening computed tomography (CT) and in order to reduce frequency of follow-up high-resolution CT (HRCT).

**Materials and Methods:** We evaluated 238 screening-detected benign lesions and 23 screening-detected lung cancers for 12 characteristics: spiculation, well-defined margin, concave margin, polygonal shape, notch/lobulation, solid component, ground-glass opacity (GGO), air bronchogram, cavity, bubble-like appearance, pleural indentation, and vascular convergence. We also measured the lesion diameters to set a threshold for benign lesions. We tested combinations of these characteristics to differentiate benign lesions from lung cancers.

**Results:** By using certain combinations of the characteristics that showed statistically significant differences between benign lesions and lung cancers, benign lesions could be extracted without contamination by lung cancer in screening CT, when the combination included solid component as a positive finding. In HRCT, more than 80% of the benign lesions could be extracted without contamination by lung cancer when the combination included GGO as a negative finding.

**Conclusion:** It seems possible to reduce the frequency of follow-up HRCT to establish a diagnosis of benign lesions using certain combinations of the characteristics of benign nodules.

**Key words:** lung cancer, screening CT, benign lesions, false positive

### INTRODUCTION

IN MASS SCREENINGS, COMPUTED TOMOGRAPHY (CT) IS much more sensitive than chest X-ray in detecting lung cancer.<sup>1-7</sup> Screening CT can detect lung cancers at earlier stages than can screening chest X-rays.<sup>1-7</sup> On the other hand, since no effective differentiator between benign nodule and lung cancer has been proposed in screening CT, it detects far more benign nodules (false positives) than screening chest X-rays.<sup>8,9</sup> In fact, the majority of pulmonary nodules detected in CT screening are not lung cancers.<sup>4,9</sup> Therefore, invasive diagnostic procedures for all detected pulmonary lesions cannot

be justified. Instead, if screening CT reveals a pulmonary lesion suspected to be lung cancer, diagnostic chest CT with high-resolution CT (HRCT) of the lesion is recommended. If HRCT does not show benign calcification in the lesion, further investigation is recommended, depending on lesion size. Henschke *et al.* reported that, with their protocol, pulmonary nodules detected in CT screening could be managed with little use of invasive diagnostic procedures.<sup>4</sup> To detect growth, that protocol recommends periodic follow-up HRCT or biopsy examination, depending on nodule size.<sup>4</sup> However, to confirm a diagnosis of benign nodule according to the stability of the nodule, follow-up CT is necessary several times for up to 2 years. Since these follow-up CTs are routine practice and are supported by health insurance in Japan, it is preferable and more cost-effective to reduce the false-positive rate in CT screening. If screening CT findings can rule out lung cancer with a reasonable false-negative rate, we can reduce the screening CT false-positive rate. Otherwise, based on the HRCT characteristics of benign nodules,<sup>10</sup> it may be possible to rule out lung cancer at the first

---

Received January 7, 2004; revision accepted February 21, 2004.  
Department of Radiology, Ehime University School of Medicine  
Reprint requests to Tadashi Murakami, M.D., Department of  
Radiology, Ehime University School of Medicine, Shitsukawa,  
Toon-city, Ehime 791-0295, JAPAN.

A part of this paper was presented at the 61st Annual Meeting of  
the Japan Radiological Society in 2002.

## HRCT examination.

The purpose of the present study was to identify the characteristics of benign pulmonary lesions on screening CT and HRCT, which may reduce the false-positive rate in CT screening or the frequency of diagnostic CT in hospitals. We retrospectively evaluated the results of screening CT and of the first HRCT of cases whose pulmonary lesions were suspicious for lung cancer and for which diagnoses had been established.

### MATERIALS AND METHODS

From December 1999 to March 2003, 16,735 individuals aged over 40 years participated in a mass screening program for lung cancer by mobile spiral CT, which was provided by the Ehime General Health Association. Positive results indicative of lung cancer were found in 2,033 participants (12.1%). Among them, we recruited 195 individuals whose diagnosis had been established and whose screening CT and HRCT were available for this study. Six were excluded from the study because the lesion was acute pneumonia and the shape differed between the screening CT and the HRCT. Finally, the CT images of 189 individuals were analyzed. The mean age was 61 years (range, 42-80 years). In 22 patients (8 men and 14 women), the pulmonary lesion was diagnosed as lung cancer. In the other 167 patients (79 men and 88 women), the pulmonary lesion was diagnosed as benign. The total number of pulmonary lesions was 23 in the lung-cancer patients (one patient had two lung cancers) and 238 in the benign-lesion patients. In all lung-cancer patients, the diagnosis was histopathologically established by surgery. The type of lung cancer was adenocarcinoma in 22 lesions and squamous cell carcinoma in the remaining lesion. Out of 22 adenocarcinomas, the classification of Noguchi was mentioned in seven: type A, 4; type B, 1; type C, 2. The stage of lung cancer was IA in 20 patients, IB in one patient, and IIB in one patient. In the one patient with double-primary cancer (adenocarcinomas), the stage was IB. The diagnoses of a majority of benign lesions were clinically established. Twenty-five lesions showed benign calcification on the HRCT image. During the two-year follow-up period, 209 solid nodules were stable. One lesion was diagnosed as pneumonia because it was improved by the administration of antibiotics. Of the three patients with hamartoma, two were histopathologically diagnosed by biopsy, and the other was diagnosed as having a fat component on the HRCT image (Table 1).

The screening CT was performed with a mobile CT van (Asterion VR, Toshiba Medical Systems, Tokyo). Low-dose spiral CT scanning of the chest was performed

with the following parameters: 120 kVp, 25 to 50 mA, 10-mm collimation, 20-mm table speed/rotation. CT images of the entire lung region were obtained in a single, 15- to 20-second breath-hold. The CT images were reconstructed at 10-mm intervals by using a high-frequency algorithm. The image data from the mobile CT were registered in a data-storage system and transferred to a dedicated workstation (RS-252, Konica Co., Tokyo). We interpreted these images at lung window settings (window width 1,600 HU, window level -600 HU) on a monitor with an 8-bit frame memory.

HRCT of the pulmonary lesions was performed with various scanners at the referred hospitals. Although the scan parameters differed among the hospitals, basically both the collimation and reconstruction interval were 1.0-2.0 mm. All image data were reconstructed with a high-frequency algorithm (lung or bone algorithm) and printed on films at lung window settings (window width 1,600 HU, window level -600 HU). We interpreted these images on a view box.

Reading tests were performed separately between screening CT and HRCT. In screening CT, all 238 pulmonary lesions were interpreted because detection of the calcification was impossible. In HRCT, 213 pulmonary lesions without benign calcification were interpreted because a diagnostic workup was terminated whenever a benign calcification was found. In each test, CT images with benign lesions and lung cancers were mixed and interpreted in random order. Three chest radiologists (M.U., S.Y., Y.Y.) interpreted the images and reached a consensus. They did not know the diagnoses of the pulmonary lesions or the patients' clinical information. They also did not know the ratio of benign lesions to lung cancers. They evaluated each pulmonary lesion according to the 12 characteristics that are reported to be useful in differentiating peripheral pulmonary lesions: spiculation, well-defined margin, concave margin, polygonal shape, notch/lobulation, solid component, ground-glass opacity (GGO), air bronchogram, cavity, bubble-like appearance, pleural indentation, and vascular convergence.<sup>10,11</sup> A well-defined margin represents a pulmonary lesion demarcated by a sharp margin from the surrounding lung parenchyma. A concave margin represents a pulmonary lesion with linear or concave sides. A polygonal shape represents a lesion surrounded by a concave margin. The observers rated each pulmonary lesion on the 12 characteristics, assigning a confidence level to each finding as follows: 4, definitely exists; 3, probably exists; 2, probably absent; 1, definitely absent (Figs. 1 and 2).

They recorded the size of each pulmonary lesion by measuring the long axis diameter at the largest section of the pulmonary lesion. In the screening CT, we

Table 1. Summary of materials

	Benign lesions	Lung cancer
Pulmonary lesion	238 lesions in 167 cases	23 lesions in 22 cases
Male/female	79/88	8/14
Age (y.o.)	60.2±0.6	65.2±8.4
Specification	No change: 234 Hamartoma: 3 Pneumonia: 1	Adenocarcinoma: 22 Sq*: 1  Stage IA: 20 IB: 1 IIB: 1

\* Sq: squamous cell carcinoma

evaluated the accuracy of this measurement by categorizing the pulmonary lesions into three groups (lesions smaller than or equal to 5 mm,<sup>4</sup> 8 mm,<sup>9</sup> and 10 mm<sup>4</sup>) based on the HRCT results to set a threshold for diagnosing a benign lesion.<sup>4,9</sup> This analysis was performed using lesions without calcification (236 lesions).

To find the characteristics of benign lesions, we compared the frequency of the 12 characteristics and the size differences between the benign lesions and the lung cancers. Then, we tested a combination of the items whose frequencies had differed significantly between the benign lesions and the lung cancers, providing an effective differentiator. We separately analyzed the results in screening CT and HRCT. In this trial, positive findings received scores of 3 or 4 while negative findings were scored 1 or 2. We also performed multivariate analysis to confirm the most effective differentiator between benign lesion and lung cancer.

The Mann-Whitney U-test and Student's t-test were used to compare findings from the screening CT with those of HRCT. A *p* value of less than 0.05 was regarded as statistically significant.

## RESULTS

In screening CT, spiculation ( $p < 0.05$ ), GGO ( $p < 0.01$ ), air bronchogram ( $p < 0.01$ ), bubble-like appearance ( $p < 0.01$ ), pleural indentation ( $p < 0.01$ ), and vascular convergence ( $p < 0.01$ ) were statistically more frequent in lung cancers than in benign lesions. Solid component ( $p < 0.01$ ) and polygonal shape ( $p < 0.05$ ) were statistically more frequent in benign lesions than in lung cancers. There were no significant differences between benign lesions and lung cancers in notch/lobulation, well-defined margin, concave margin, and cavity. The lung cancers were on average significantly larger than the benign lesions [ $17.0 \pm 9.2$  mm (5-42 mm) vs.  $6.6 \pm 2.8$

mm (3-21 mm), respectively] (Fig. 3).

In HRCT, spiculation ( $p < 0.01$ ), GGO ( $p < 0.01$ ), air bronchogram ( $p < 0.01$ ), bubble-like appearance ( $p < 0.01$ ), vascular convergence ( $p < 0.01$ ), notch/lobulation ( $p < 0.01$ ), and pleural indentation ( $p < 0.01$ ) were statistically more frequent in lung cancers than in benign lesions. Solid component ( $p < 0.01$ ), polygonal shape ( $p < 0.01$ ), and well-defined margin ( $p < 0.01$ ) were statistically more frequent in benign lesions than in lung cancers. There were no significant differences in concave margin and the presence of cavities between benign lesions and lung cancers. The lung cancers were on average significantly larger than the benign lesions [ $17.0 \pm 9.3$  mm (4-35 mm) vs.  $6.6 \pm 2.5$  mm (3-18 mm), respectively] (Fig. 4).

The numbers of pulmonary lesions with below-threshold diameters in HRCT were distributed as follows: smaller or equal to 5 mm, 84 (81 benign lesions, 3 lung cancers) (36%); 8 mm, 191 (185 benign lesions, 6 lung cancers) (81%); 10 mm, 205 (198 benign lesions, 7 lung cancers) (87%). In the screening CT, the numbers of pulmonary lesions with below-threshold diameters were distributed as follows: 5 mm, 82 (80 benign lesions, 2 lung cancers) (35%); 8 mm, 186 (182 benign lesions, 4 lung cancers) (79%); 10 mm, 203 (197 benign lesions, 6 lung cancers) (86%). Between screening CT and HRCT, there was no significant difference in the number of pulmonary lesions under each threshold. However, 24% (20/82) of the lesions below the threshold of 5 mm in the screening CT actually had diameters of greater than 5 mm in HRCT. On the other hand, 97% of the lesions below the threshold of 8 mm and 96% of the lesions below the threshold of 10 mm were identical between the screening CT and HRCT. Thus, we decided to make 8 mm the threshold diameter of benign lesions in the following study.

We used the combination of size threshold and items that had statistically significant differences between lung

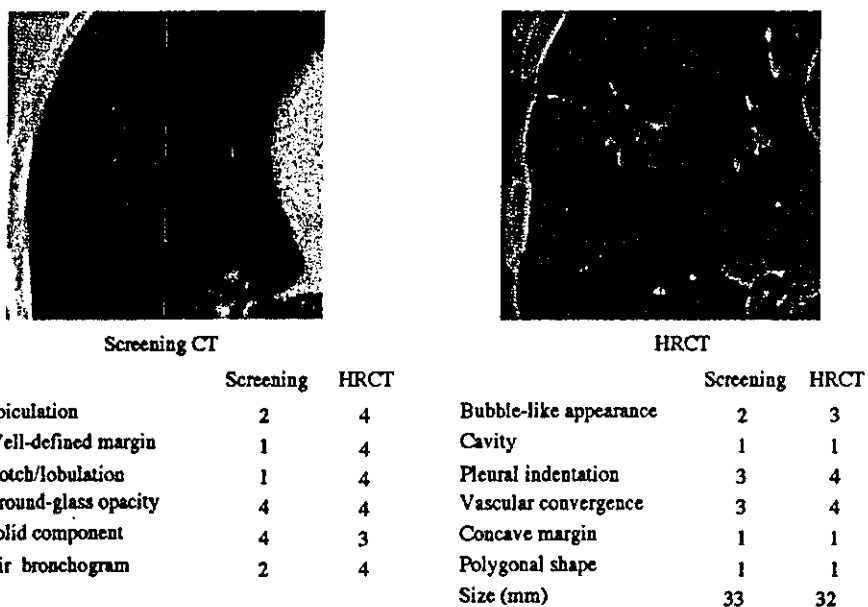


Fig. 1. A 75-year-old woman with lung cancer (adenocarcinoma, stage IA). In screening CT, the margin of the lesion was blurred. It was difficult to recognize spiculation, notch/lobulation, and air bronchogram. The respective confidence ratings for these were 1, 2, and 2. In HRCT, all the scores were 4.

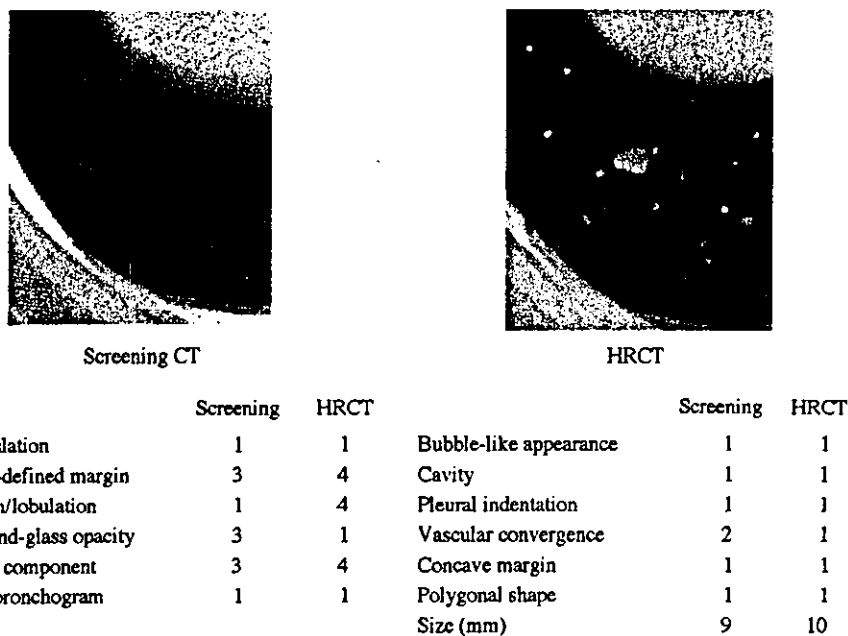
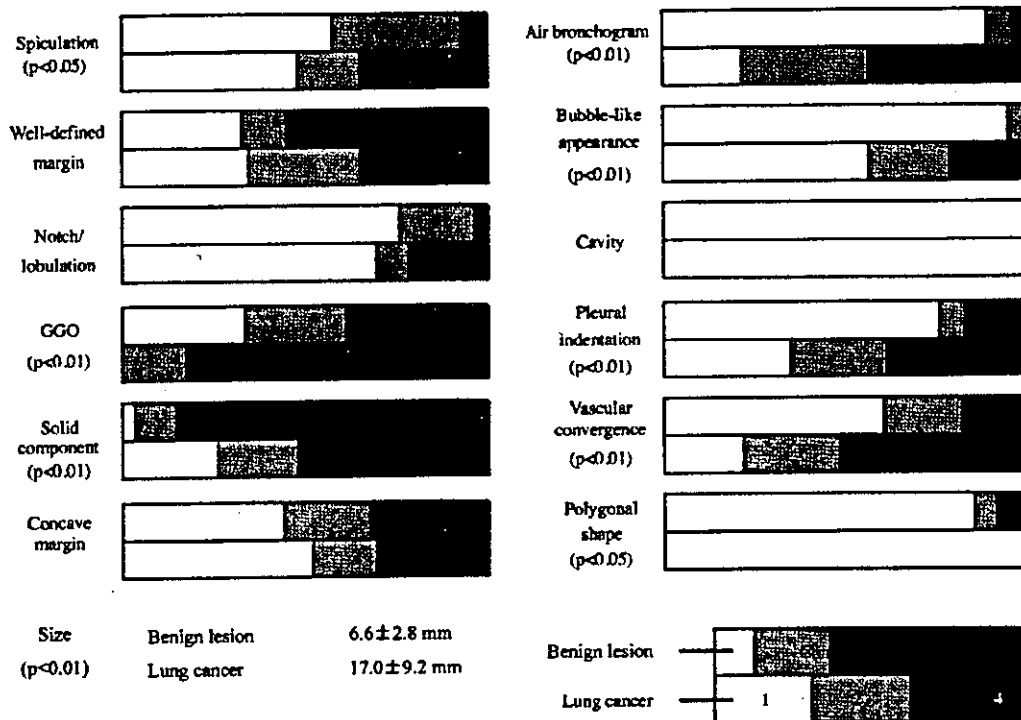


Fig. 2. A 43-year-old woman with hamartoma. In screening CT, the GGO score was 3 and that for notch/lobulation was 1. In HRCT, the scores were 1 and 4, respectively.



**Fig. 3.** Image analysis of benign lesions and lung cancer in screening CT. The ratio of each confidence rating is illustrated with gray scale. The confidence ratings for benign lesions appear in the upper column, and those for lung cancers are in the lower column. The confidence ratings for spiculation, ground-glass opacity (GGO), air bronchogram, bubble-like appearance, pleural indentation, and vascular convergence were significantly higher in lung cancers than in benign lesions. On the other hand, the ratings for solid component and polygonal shape were significantly higher in benign lesions than in lung cancer. The lung-cancer lesions were significantly larger than the benign lesions.

cancers and benign lesions in order to differentiate the benign lesions from the lung cancers. We examined 511 combinations in screening CT and 2,047 combinations in HRCT. In screening CT, it was possible to extract many benign lesions without contamination by lung cancer when the combination included solid component. Otherwise, when lesions had polygonal shape, 22 benign lesions were extracted without contamination by lung cancers. The other combinations were contaminated by some lung cancers. Table 2 summarizes the top six combinations of items in which many benign lesions were extracted without contamination by lung cancers. When the differentiator was a combination of solid component and  $\leq 8$  mm; solid component without spiculation and without vascular convergence; solid component without GGO and without air bronchogram; solid component without GGO and without pleural indentation; solid component without GGO and without vascular convergence; and with polygonal shape, 198 benign lesions out of 238 (83.2%) could be extracted without contamination by lung cancer. On the other hand, in HRCT, in some combinations with GGO, we could

also extract many benign lesions without contamination by lung cancers. Otherwise, when lesions had polygonal shape, we could extract 32 benign lesions without contamination by lung cancers. However, the other combinations were contaminated by some lung cancers. Table 3 summarizes the top 10 combinations of items in which many benign lesions were extracted without contamination by lung cancers. When the differentiator was one of the following combinations: without GGO and without spiculation; without GGO and without air bronchogram; without GGO and without bubble-like appearance; without GGO and without notch/lobulation; without GGO and without pleural indentation; without GGO and without vascular convergence; without GGO and  $\leq 8$  mm; and with polygonal shape, 204 benign lesions out of 213 (95.8%) could be extracted without contamination by lung cancer.

Results of the multivariate analysis were as follows. In screening CT, statistically significant parameters were with solid component ( $p=0.010$ , odds ratio=12.4), without air bronchogram ( $p=0.046$ , odds ratio=5.5), and  $\leq 8$  mm ( $p=0.001$ , odds ratio=10.4). In HRCT, we



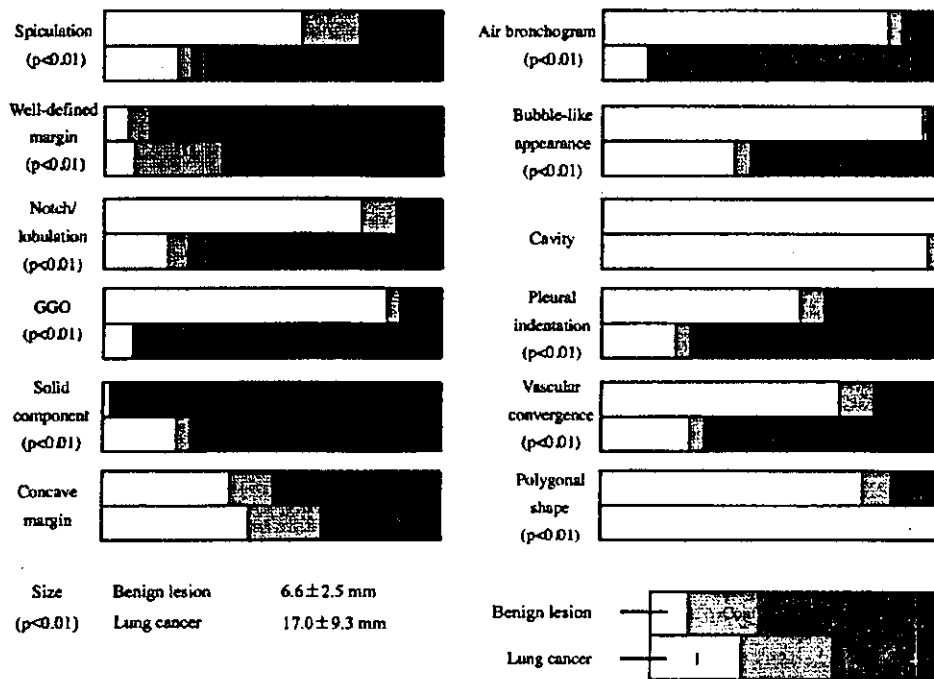


Fig. 4. Image analysis of benign lesions and lung cancer in HRCT.

The ratio of each confidence rating is illustrated with gray scale. The confidence ratings for benign lesions appear in the upper column, and those for lung cancer are in the lower column. The confidence ratings for spiculation, notch/lobulation, ground-glass opacity (GGO), air bronchogram, bubble-like appearance, pleural indentation, and vascular convergence in lung cancer were significantly higher than in benign lesions. On the other hand, the ratings for solid component, well-defined margin, and polygonal shape were significantly higher in benign lesions than in lung cancers. The lung cancer lesions were significantly larger than the benign lesions.

excluded well-defined margin from multivariate analysis, since GGO and well-defined margin were in reciprocal relation. The statistically significant parameters were without notch/lobulation ( $p=0.013$ , odds ratio=86.2), without GGO ( $p=0.048$ , odds ratio=61.0), and with solid component ( $p=0.012$ , odds ratio=142.9).

### DISCUSSION

In this study, we proposed some differentiators between benign lesion and lung cancer in screening CT and HRCT. The frequency of a polygonal shape, which is regarded as a characteristic of benign lesions,<sup>10</sup> was significantly higher in the benign lesions, as no lung cancers had this shape. The absence of polygonal-shaped lung cancers in this study confirmed that this item was discriminative of benign lesions. However, the sensitivity of the polygonal shape (15%, 32/213) was not high enough to allow differentiation between the benign lesions and the lung cancers. The absence of characteristics of peripheral adenocarcinoma such as

spiculation, GGO, air bronchogram, bubble-like appearance, pleural indentation, and vascular convergence were important to differentiate benign lesions from lung cancers. This was compatible with the fact that 22 of the 23 lung cancers were adenocarcinomas in this study. Using the combination of these characteristics, we could extract many benign lesions both in screening CT and in HRCT without contamination of lung cancer. Since other screening CT studies also reported that the majority of the detected lung cancers were adenocarcinomas,<sup>1,2</sup> we consider that these differentiators will be universally useful in lung cancer screening with CT.

On the other hand, some types of lung cancers that we did not find in this series of patients, for example, peripheral small cell carcinoma, do not have the characteristics that are common in peripheral adenocarcinoma.<sup>12</sup> Using the above-mentioned differentiators, these types of cancer may be misdiagnosed as benign lesions. At the moment, according to the recommendation for pulmonary lesions found in screening CT, a lesion larger than or equal to 1 cm basically requires

Table 2. Screening CT findings and detected benign lesions

GGO	AB	PI	VC	Sp	Size*	PS	So	Benign lesions (n=238)	Lung cancer (n=23)
					P		P	167 (70%)	0
			N	N			P	156 (66%)	0
N	N						P	143 (60%)	0
N		N					P	125 (53%)	0
N			N				P	122 (51%)	0
						P		22 (9%)	0

P: positive, N: negative

AB: air bronchogram, GGO: ground-glass opacity, PI: pleural indentation, PS: polygonal shape, So: solid component, Sp: spiculation, VC: vascular convergence

\*smaller than or equal to 8 mm in diameter

Table 3. HRCT findings and detected benign lesions

GGO	BLA	AB	N	VC	Sp	PI	Size*	PS	Benign lesions (n=213)	Lung cancer (n=23)
N	N								183 (86%)	0
N		N							181 (85%)	0
N			N						172 (81%)	0
N							P		167 (78%)	0
N				N					158 (74%)	0
N					N				150 (70%)	0
N						N			124 (58%)	0
								P	32 (15%)	0

P: positive, N: negative

AB: air bronchogram, BLA: bubble-like appearance, GGO: ground-glass opacity, N: notch/lobulation, PI: pleural indentation, PS: polygonal shape, Sp: spiculation, VC: vascular convergence

\*smaller than or equal to 8 mm in diameter

histopathological diagnosis. Considering these conditions, although the frequency of such a situation may be low based on the results of this study and previous reports,<sup>4</sup> it may be safe to apply our differentiator to lesions whose diameter is below 1 cm. The frequency of misdiagnosis should be confirmed by a prospective study before applying these differentiators to screening CT and HRCT.

The most effective differentiators for extracting benign lesions were solid component in screening CT and GGO in HRCT. These were also indicated as statistically significant parameters in the multivariate analysis. We consider that the difference between screening CT and HRCT was caused by the difference in the spatial resolution of images. Although the spatial resolution of screening CT is far lower than that of HRCT,<sup>13</sup> solid component was demonstrated by HRCT in 213 of 216 pulmonary lesions that were judged to have a solid component in screening CT. On the other

hand, in screening CT, GGO was missed in three lung cancers that were judged to have GGO in HRCT. These facts indicate that we cannot simply apply differentiators that are effective in HRCT to screening CT.

Lesions detected by CT screening for lung cancer can be managed with some certainty according to their size.<sup>4</sup> We chose 8 mm as the threshold to extract benign lesions based on previous reports<sup>9</sup> and the measurement test. In a Mayo Clinic study, Swensen *et al.* found 2,832 non-calcified nodules in 69% of 1,049 participants.<sup>9</sup> Those lesions were found to contain 40 lung cancers (1.4%). Thus, 98.6% of detected lung nodules were benign. Among the total, 2,685 nodules (95%) were less than 8 mm, and these included eight lung cancers. Of the eight, two were detected only by sputum cytology. As a result, 99.8% (2,679/2,685) of CT-detected nodules of less than 8 mm were identified as benign. Yokouchi *et al.* reported the frequency of lymph-node metastases among surgical cases of small adenocarcinomas.<sup>14</sup> Although 9.2% had

lymph-node metastasis when the tumor was 11 mm to 15 mm, 24.3% had lymph-node metastasis when the tumor was 16 mm to 20 mm. This indicates that if we can find lung cancer of less than 15 mm, it will be at an early stage. Hasegawa *et al.* reported the relationship between a tumor's appearance on HRCT and its doubling time.<sup>15</sup> They categorized tumors in three ways, according to HRCT appearance: GGO, focal GGO with a solid central component, and solid nodule. Their respective mean doubling times were 813 days, 457 days, and 149 days. The solid nodule type consisted of rapid-growing solid tumors such as squamous cell carcinomas and small cell carcinomas. These reports suggest a considerable chance to cure such cancers, since lung cancers that are missed at 8 mm do not, even in the worst cases, exceed 15 mm when screened one year later. This projection would support our choosing 8 mm as the threshold. To introduce this idea to CT screening, we have to determine the relationship between the size of lung cancers other than adenocarcinoma and the speed at which they progress. To solve this problem, much effort must be applied to clarify the biological history of small lung cancers.

This study had some limitations. First, since CT screening for lung cancer is a rapidly advancing field, techniques are improving day by day. Swensen *et al.* have already used multi-detector row CT in their screening program.<sup>9</sup> Their screening CT would likely have higher spatial resolution than ours, as well as greater recognition of pulmonary lesion characteristics that approaches the recognition of HRCT in this study. It may be possible to apply the differentiators that are effective in HRCT directly to screening CT with multi-detector row CT.

Second, because of the limited number of lung cancers, we could not perform this analysis to include categorizing the lesions by size. There may be a difference in differentiator between small and large lesions because the appearance of lung cancer could change according to its growth. Although we think this study provided useful clues to diagnosing benign lesions, more detailed analyses with larger populations of patients will permit some arrangement of differentiators according to the size of lesions.

Third, since this study was retrospective, there is likely some bias in the selection of pulmonary lesions. The incidence of lung cancer was far greater in our cases than in the actual population. Although the trend of the extraction ratio of benign lesions to cancerous contamination should be correct in this study, the ratio in the real population should be reexamined in a prospective study.

In conclusion, the present study indicated the

possibility of extracting benign lesions by combining certain characteristics of pulmonary lesions along with a threshold lesion size in screening CT. We consider that since extraction was more reliable in HRCT, it is possible that the first HRCT can establish diagnoses of certain numbers of benign lesions.

#### ACKNOWLEDGMENTS

The authors thank Professor Kenji Eguchi, Division of Pulmonary Medicine, Tokai University, School of Medicine; Dr. Nobuo Ueda, Department of Internal Medicine (For Respiratory Disease), Ehime Prefectural Central Hospital; Dr. Kazutaka Nishimura, Department of Internal Medicine, Ehime National Hospital; Dr. Hiroshi Mogami, Department of Radiology, Shikoku National Cancer Center; and Dr. Masamitsu Yamaizumi, Department of Radiology, Ehime National Hospital, Dr. Toshiaki Kawakami, and Dr. Shigeo Ooishi, Ehime General Health Association, for their thoughtful mentorship and encouragement of young radiologists as members of the Ehime Anti-Lung Cancer Organization, an organization consisting of doctors, technicians, physicists, and other staff involved in mass screening for lung cancer in Ehime Prefecture.

#### REFERENCES

- 1) Kaneko M, Eguchi K, Ohmatsu H, *et al.* Peripheral lung cancer: screening and detection with low-dose spiral CT versus radiography. *Radiology*, 201: 798–802, 1996.
- 2) Sone S, Takashima S, Li F, *et al.* Mass screening for lung cancer with mobile spiral computed tomography scanner. *Lancet*, 351: 1242–1245, 1998.
- 3) Sone S, Li F, Yang ZG, *et al.* Characteristics of small lung cancers invisible on conventional chest radiography and detected by population based screening using spiral CT. *Br J Radiol*, 73: 137–145, 2000.
- 4) Henschke CI, McCauley DI, Yankelevitz DF, *et al.* Early lung cancer action project: overall design and findings from baseline screening. *Lancet*, 354: 99–105, 1999.
- 5) Henschke CI, Miettinen OS, Yankelevitz DF, *et al.* Radiographic screening for cancer. Proposed paradigm for requisite research. *Clin Imaging*, 18: 16–20, 1994.
- 6) Ohmatsu H, Kakinuma R, Kaneko M, *et al.* Successful lung cancer screening with low-dose helical CT in addition to chest x-ray and sputum cytology: the comparison of two screening periods with or without helical CT (abstr). *Radiology*, 217: 242, 2000.
- 7) Diederich S, Wormanns D, Lenzen H, *et al.* Screening for early lung cancer with low-dose computed tomography of the chest: results of baseline examinations in 919 asymptomatic smokers. *Eur Radiol*, 10: S253, 2000.
- 8) Sone S, Li F, Yang Z, *et al.* Diagnostic workup of CT-screening positive cases: attainable performance; Japan

- perspective. Article written for First International Conference on Screening for Lung Cancer, 1999.
- 9) Swensen SJ, Jett JR, Hartman TE, *et al.* Lung cancer screening with CT: Mayo Clinic experience. *Radiology*, 226: 756–761, 2003.
  - 10) Takashima S, Sone S, Li F, *et al.* Small solitary pulmonary nodules ( $\leq 1$  cm) detected at population-based CT screening for lung cancer: reliable high-resolution CT features of benign lesions. *AJR Am J Roentgenol*, 180: 955–964, 2003.
  - 11) Zwirwich CV, Vedal S, Miller RR, *et al.* Solitary pulmonary nodule: high-resolution CT and radiologic-pathologic correlation. *Radiology*, 179: 469–476, 1991.
  - 12) Yabuuchi H, Murayama S, Sakai S, *et al.* Resected peripheral small cell carcinoma of the lung: computed tomographic-histologic correlation. *J Thorac Imaging*, 14: 105–108, 1999.
  - 13) Itoh S, Ikeda M, Arahata S, *et al.* Lung cancer screening: minimum tube current required for helical CT. *Radiology*, 215: 175–183, 2000.
  - 14) Yokouchi H, Kodama K, Higashiyama M, *et al.* Diagnosis and treatment of small peripheral lung cancer. *Nippon Rinsho*, 58: 1142–1148, 2000. (in Jpse.)
  - 15) Hasegawa M, Sone S, Takashima S, *et al.* Growth rate of small lung cancers detected on mass CT screening. *Br J Radiol*, 73: 1252–1259, 2000.